Characterization and exploitation of heterogeneous OFDM primary users in cognitive radio networks

Anna Vizziello · Ian F. Akyildiz · Ramon Agustí ·
Lorenzo Favalli · Pietro Savazzi

Abstract The fundamental features of cognitive radio (CR) systems are their ability to adapt to the wireless environment where they operate and their opportunistic occupation of the licensed spectrum bands assigned to the primary network. CR users in CR systems should not cause any interference to primary users (PUs) of the primary network. For this purpose, CR users need to accurately estimate the features and activities of the primary users. In this paper, a novel characterization of heterogeneous PUs and a novel reconfigurability solution in CR networks are introduced. The characterization of PUs consists of a detector and classifier that distinguishes between heterogenous PUs. The PU characteristics stored in radio environmental maps are utilized by an interference/throughput adapter for the optimization of CR parameters. The performance of the proposed solutions is evaluated by showing false alarm and missed detection probabilities of the detector/classifier in a multipath fading channel with additive white Gaussian noise. Moreover, the impact of the PU characteristics on the CR throughput is analyzed.

Keywords Spectrum sensing · Signal classification · Interference protection · Throughput · Cognitive radio networks

A. Vizziello (✉) · L. Favalli · P. Savazzi
Dipartimento di Ingegneria Industriale e dell'Informazione,
Università degli Studi di Pavia, Via Ferrata 1, 27100 Pavia, Italy
e-mail: anna.vizziello@unipv.it

L. Favalli
e-mail: lorenzo.favalli@unipv.it

P. Savazzi
e-mail: pietro.savazzi@unipv.it

I. F. Akyildiz
Telecommunication Engineering School (ETSETB),
Universitat Politècnica de Catalunya, C. Jordi Girona 31,
08034 Barcelona, Spain
e-mail: ian@ac.upc.es

I. F. Akyildiz
Department of Information Technology, King Abdulaziz
University, Jeddah, Saudi Arabia

R. Agustí
Department of Signal Theory and Communications (TSC),
Universitat Politècnica de Catalunya, C. Jordi Girona 31, 08034
Barcelona, Spain
e-mail: ramon@tsc.upc.edu

1 Introduction

Nowadays wireless networks are characterized by a fixed spectrum assignment policy, i.e. the spectrum is regulated by governmental agencies and it is assigned to license holders or services. However, observations reveal that portions of this spectrum are used sporadically in any given location [4]. The current inefficient spectrum usage calls for a new networking paradigm based on more flexible opportunistic utilization of the available spectrum. Cognitive radio (CR) is envisaged as the key enabling solution to solve these current spectrum inefficiency problems.

The cognitive radio paradigm allows CR users to detect, use and share the available spectrum, so that the licensed or primary users (PUs) are unaffected [1, 5]. In particular, a CR can occupy the band under the condition that it has to vacate the spectrum as soon as the primary user (PU) is detected. Alternatively, both PU and CR can use that same

spectrum band as long as the CR limits the interference towards PU to tolerable levels.

To this purpose, a CR must identify active PUs and spectrum holes, also called white spaces, and this is obtained through CR spectrum sensing capability. Among all sensing techniques, feature detection [11] has recently gained attention due to its better immunity to noise uncertainty with respect to other approaches.

As an example, orthogonal frequency division multiplexing (OFDM) signals exhibit periodicities embedded in equally spaced sinusoidal carriers, cyclic prefix and pilot sequences [2]. These periodicities can be exploited by a feature detector [20] to discover the presence of OFDM PU signals through the cyclostationary autocorrelation function (CAF) [11, 18] or the spectral correlation function (SCF) [2, 17].

With respect to a simple energy detector, a feature detector is also capable of discriminating signal types. In [9] the authors propose a method that uses a support vector machine to classify the received signals, improving accuracy by feature matching.

The ability to classify signals enables a better awareness of the environment and becomes crucial to mitigate the interference caused by CRs to different PUs. The allowable interference, depends in general on the primary system [15] under consideration. For example, the IEEE 802.22 standard defines specific sensing requirements, such as sensing receiver sensitivity and signal-to-noise ratio (SNR), for different PU signal types [14, 16].

Motivated by all these issues, we develop a system that takes into account heterogeneous PUs, also called PU types in the following, instead of the simple ON-OFF PU model. After distinguishing different PUs, we present a novel method to exploit PU signals classification in CR networks. This issue is not addressed in existing classification methods, such as [2].

Here, we present a novel framework named Characterization of heterogeneous PUs and Reconfigurability effects in CR networks $(CR)^2$. The main original contributions of this framework are:

- *Characterization of heterogeneous PUs*. The core of this module is a *cyclostationary feature (CF) detector/classifier* for OFDM signals. A novel test statistic is proposed to detect and classify PU signals, according to a new PU activity model [3] integrated in the scheme. This is more accurate than the commonly used Poisson model because it considers correlations and similarities within data. Then, for each PU type the following features are extracted: *allowed interference threshold*, *bandwidth* and *idle/busy time*. These features are stored in radio environmental maps (REMs) database.
- *CR reconfigurability*, which basically consist of a *throughput adapter* that exploits the PU features stored

in REMs for a better tuning of CR parameters in different scenarios. Moreover, we consider that each PU type allows a different interference level. In this way, an adaptive interference protection is introduced by changing CR transmission power.

The remainder of the paper is organized as follows: in Sect. 2 the network architecture and the modules of the proposed $(CR)^2$ framework are presented. In particular, the blocks of the *characterization of heterogeneous PUs* are described in Sect. 3, while the modules concerning *CR reconfigurability* are shown in Sect. 4. In Sect. 5 the system performance is evaluated by showing the probability of false alarm and missed detection of the *CF detector/classifier*, and the impact of PU features on CR throughput; finally, the conclusions are presented in Sect. 6.

2 System model and network architecture

We assume OFDM-based primary systems, as employed by several modern PU standards, and an infrastructure-based CR network with a centralized entity such as a CR base station. According to this scenario, CRs send sensing information to a CR base station for processing and storing it in a REM database. This information is then broadcasted within the CR network for throughput adaptation.

In particular, REMs have been proposed as integrated databases that provide an abstraction of the radio environment conditions [21]. REMs are used to obtain the required geo-localized spectral activities, policy information, propagation models and other radio frequency (RF) environment information, which are then used to estimate the available spectrum resources. A REM covers multi-domain environmental information such as geographical features, available services, spectral regulations, location of diverse entities of interest (e.g., radios, reflectors, obstacles) as well as radio equipment capability profiles, relevant policies and past experiences.

The stored information can be updated with observations from CRs and disseminated throughout CR networks. Here we assume that, after the classification of heterogeneous PUs, information about PU features is obtained via a REM database. The way of disseminating such information is not the focus of this paper and more details can be found in [19].

In the following, we consider a CR that is sensing the channel to investigate the presence of PUs. Specifically, we take into account heterogeneous PU signals specified in distinct standards, which are characterized by different values of OFDM parameters, such as guard interval length, symbol duration, and subcarrier spacing.

Let y be the total signal received by the CR during its sensing operation, and let y_j be the contribution due to the

transmission of the *j*-th PU type. In particular, here we consider that PU signals transmit on different frequencies, thus they are orthogonal and do not cause interference on the contribution of another PU signal.

Let H_0 and H_1 represent respectively the hypothesis that the *j*-th PU type is inactive and active. Under each hypothesis, the *i*-th time sample of the *j*-th received signal y_j at the CR device is given by

$$y_j(i) = \begin{cases} w(i) & H_0 \\ \sum_{l=0}^{L-1} h_l x_j(i-l) + w(i) & H_1 \end{cases} \tag{1}$$
$$\forall i \in [1, 2, \ldots, p]$$

where *p* is the total number of time samples. The PU signal $x_j(i)$ is an independent and identically distributed (*iid*) random process with mean μ_{x_j} and variance $E\left[|x_j(i)^2|\right] = \sigma_{x_j}^2$. $w(i)$ is the additive white gaussian noise (AWGN) with zero mean and variance $E\left[|n(i)^2|\right] = \sigma_n^2$. In (1), a multipath fading channel [13] is assumed, and h_l is the complex envelope of the *l*-th propagation path with delay time *l* normalized to the sampling period, with $0 \le l < L$.

Figure 1 shows an overview of the proposed $(CR)^2$ framework along with its modules. As depicted in the figure, we consider heterogeneous PUs instead of the simple ON-OFF PU model. In the *PUs characterization* frame we extract the useful information that are then exploited for *CR reconfigurability*. In this way, we obtain an improvement of CR adaptability and a more efficient use of the available spectrum resources.

Figure 1 also highlights the input/output connections of the modules of the $(CR)^2$ framework. Going in more detail, the *PUs characterization* consists of three blocks: *PU activity model*, *CF detector/classifier*, and *PU features module*; and the *CR reconfigurability* contains *CR adaptive parameters* and *CR throughput adapter*.

The time domain vector $y_j(i)$ shown in Fig. 1 is the signal of the *j*-th PU type monitored by CRs and it is the input of the proposed scheme. $y_j(i)$ is used in the *PU activity model* block to extract the PU activity index [3], which is a more accurate metric than the Poisson modeling. The received signal $y_j(i)$ is also the input of the *CF detector/classifier*, which has the ability to classify PU signals. After distinguishing PU signal types and activities, in the *PU features module*, several features of PUs are extracted in order to adaptively increase CR throughput. The throughput is calculated in the block *CR throughput adapter* according to *CR adaptive parmeters*, which are strictly connected to the features of the detected PU types. Actually, CR throughput depends on PU allowed interference levels, bandwidth and idle/busy time, whose values vary depending on the detected PU types. Thus, by considering heterogeneous PUs with several features, we have greater CR transmission opportunities than with a simple ON-OFF PU model.

3 Characterization of heterogeneous PUs

In this section, the first group of modules shown in Fig. 1 are described in details.

3.1 Primary users activity model

It is known that the performance of a CR network is related to PU activity, therefore a precise model of PU activity is useful to characterize the spectrum availability.

The model proposed in [3] follows the spiky fluctuations of PU traffics over time, accurately modeling the PU activity and thus overcoming the drawbacks of the usual Poisson characterization. As shown in Fig. 1, the PU activity model [3] is integrated in the proposed scheme.

The model consists of three steps. In the first step, the modeled PU signal is organized in clusters according to the

Fig. 1 Modules of the system for the $(CR)^2$ framework
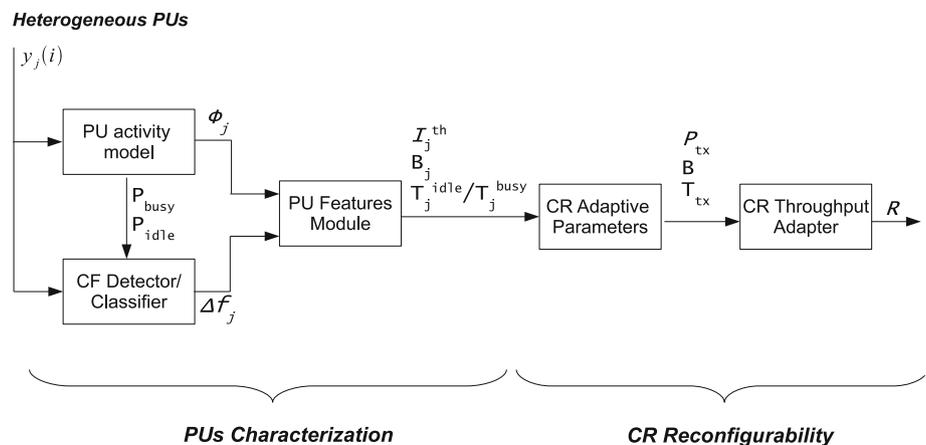
first-difference clustering scheme. In the second step, a temporal correlation among modeled PU samples is carried out. In the last step, a new activity index, called *primary user activity index* $\phi_j(i)$, is derived to capture the PU activity fluctuation taking into account both first-difference and correlation scheme [3]:

$$
\phi_j(i) = [r_j(i) - r_j(i-1)] \times
$$
$$
\left[\left| \frac{1}{2} \sum_{q=1}^{3} \left(\frac{d(q) - E[d^{[3]}]}{\sigma_{d^{[3]}}} \right) \left(\frac{r_j(i+1-q) - E[r_j^{[3]}]}{\sigma_{r_j^{[3]}}} \right) \right| \right],
$$
$$
\forall i \in [1, 2, \ldots, p]
$$

(2)

in which the index j refers to the j-th band monitored by CR where the j-th PU type is transmitting. $r_j(i)$ is the modeled PU activity vector at the i-th time sample, $r_j^{[3]}$ is the modeled PU activity vector with three elements, $d^{[3]}$ is an index vector d with three elements, $E[\cdot]$ is the mean operator, σ is the standard deviation, p is the total number of PU activity monitoring samples. The first factor $[r_j(i) - r_j(i-1)]$ in (2) indicates that $\phi_j(i)$ captures the fluctuations and short-term spiky characteristics of the PU activity in the j-th band by using the first-difference clustering scheme proposed in [3]. The second term $\left[\left| \frac{1}{2} \sum_{q=1}^{3} \left(\frac{d(q) - E[d^{[3]}]}{\sigma_{d^{[3]}}} \right) \left(\frac{r_j(i+1-q) - E[r_j^{[3]}]}{\sigma_{r_j^{[3]}}} \right) \right| \right]$ accounts for the temporal correlation scheme proposed in [3].

P_{busy} and P_{idle} of PU activity depend on the PU model used and are computed as follows:

$$
P_{busy} = \sum_{i=1}^{p} \frac{2(r_j(i) - 2\Omega\Psi)}{2}
$$

(3)

and

$$
P_{idle} = \sum_{i=1}^{p} \frac{r_j(i) - 2\Omega\Psi}{2}
$$

(4)

where $r_j(i)$ is the modeled PU activity vector. Ω and Ψ are binary variables employed to express the temporal correlation and the correlation slope, respectively, as detailed in [3].

3.2 Cyclostationary feature (CF) detector/classifier

Detailed PU characterization becomes essential for improving spectrum awareness. For this purpose signal detection and classification functions are mandatory. In fact, a simple energy detector can only detect the presence of signal, while on the contrary, a feature detection has the ability to distinguish signals from different networks [2, 11, 17, 20]. Furthermore, differently from the energy detector, it is robust to the uncertainty of noise power, especially at

low SNR [6]. We exploit this capability to develop a system that minimizes PU interference and maximizes CR spectrum usage at the same time.

The *cyclostationary feature (CF) detector/classifier* module of Fig. 1 consists of a feature detector and a signal classifier:

3.2.1 Feature detector

The cyclostationary autocorrelation function $R_x^\alpha(\tau_s)$ of a signal x is defined as:

$$
R_x^\alpha(\tau_s) = \frac{1}{p} \sum_{i=0}^{p-1} x(i) x^*(i + \tau_s) e^{-j2\pi\alpha t_s}
$$

(5)

where α is the cyclic frequency and $\alpha \in A$. A is equal to c/T, where $c = [1, 2, \ldots]$ and T is a certain period. τ_s is the delay time τ normalized by the sampling period t_s and p is the number of samples.

In this work we use the CAF to detect PUs focusing on OFDM signals because it is employed by several modern PU standards. The CAF of an OFDM signal exhibits peaks at cyclic frequencies α equal to c/T and $\tau_s = T_u$, where T corresponds to the duration time of an OFDM block and $T_u = T - T_g$ is the data duration time. In an OFDM signal, these peaks are introduced by built-in periodicity due, for example, to cyclic prefix. In fact for a non-cyclostationary signal, such as AWGN, the CAF does not show any peak for $\alpha \neq 0$. The AWGN has a peak only for $\alpha = 0$ and $\tau_s = 0$ and we use this feature to distinguish between the presence or absence of PU signals.

For $\alpha = 0$ and $\tau_s = 0$, the feature detector is reduced to an energy detector. Choosing $\alpha = 0$ and $\tau_s \neq 0$, the feature detector becomes simpler, similar to an energy detector, but it has the additional ability of distinguishing different PU signals.

Given the received signal y_j, we define the test statistic as follows:

$$
Z_{y_j} = \max\left[R_{y_j}^0(\tau_s(i)) \right] \quad \forall \tau_s(i) \neq 0
$$

(6)

in which $R_{y_j}^0$ is the CAF of the received signal y_j, which is obtained from (5) by replacing the generic signal x with the received signal y_j, and choosing $\alpha = 0$. Since the normalized delay time τ_s is not known, its closest value is obtained by replacing τ_s in (5) with $\tau_s(i)$, where $\tau_s(i) = i \times t_s$ is normalized to the sampling time t_s. Note that the estimation of channel h_l expressed in (1) is not required in the proposed CF detector, since only the received signal y_j is used as input.

We define the decision threshold λ as the mean value of the CAF of noise R_w^0 plus and additional term ϵ, whose value is appropriately chosen to obtain a given probability of false alarm:

$$\lambda = E\left[R_w^0(\tau_s(i))\right] + \epsilon \quad \forall \tau_s(i) \neq 0 \quad (7)$$

More details on the value of ϵ are given in the discussion of the simulation results in Sect. 5.2.

After calculating Z_{y_j}, the detector makes the decision

$$\begin{cases} Z_{y_j} > \lambda & decide\, H_1 \\ otherwise & decide\, H_0 \end{cases} \quad (8)$$

A maximum a posteriori (MAP) detector is known to be optimal [13], but it requires priori knowledge of the probabilities of the *busy* and *idle* states [8, 10, 11]. For this reason, a suboptimal maximum likelihood (ML) detection is widely used as it does not require these probabilities. In our work, we propose to infer P_{busy} and P_{idle} from the PU activity model and consequently the *CF detector/classifier* module in Fig. 1 uses MAP.

In order to assess the performance of the detector it is important to evaluate its ability to correctly determine the active PUs and the white spaces. Detecting active PUs is fundamental to avoid the interference towards PUs, while correctly capturing the white spaces increases the spectrum utilization. We then calculate the probability of correct detection P_d and the probability of false alarm P_f as:

$$P_d = Pr\left[Z_{y_j} > \lambda | H_1\right] \cdot P_{busy} = \bar{P}_d \cdot P_{busy} \quad (9)$$

and

$$P_f = Pr\left[Z_{y_j} > \lambda | H_0\right] \cdot P_{idle} = \bar{P}_f \cdot P_{idle} \quad (10)$$

$\bar{P}_d$ and $\bar{P}_f$ are related to the definition of Z_{y_j} shown in (6), while P_{busy} and P_{idle}, which depend on the PU activity model, are given in (3) and (4). In particular, under H_0, Z_{y_j} follows χ_{2K}^2, where χ_q^2 is the central chi-squared distribution with q degrees of freedom. Thus, the threshold λ, given in (7), for attaining a given $\bar{P}_f$ can be calculated through the table of χ_{2K}^2.

3.2.2 Signal classifier

The periodicities of OFDM signals are useful to distinguish different PUs. In particular, we use the test statistic in (6) also to classify the signals. The CAF of the *j*-th OFDM signal exhibits a peak at cyclic frequencies α equal to c/T_j and delay time τ_s equal to T_{u_j}. The useful duration time T_{u_j} equals $1/\Delta f_j$, where Δf_j is the subcarrier spacing. This parameter depends on the PU type. Thus, we use the interval time in which the CAF exhibits the maximum to distinguish different PU signals. Specifically, we know that:

$$R_{y_j}^0(T_{u_j}) = \max\left[R_{y_j}^0(\tau_s(i))\right] \quad (11)$$

$R_{y_j}^0(\tau_s(i))$ in (11) varies for $1 < i < N_s$ where N_s is set to a predefined value.

After calculating $R_{y_j}^0(\tau_s(i))$ for $1 < i < N_s$, the value of $\tau_s^*(i)$ in which $R_{y_j}^0$ has the maximum is extracted:

$$\tau_s^*(i) : R_{y_j}^0\left(\tau_s^*(i)\right) = \max\left[R_{y_j}^0\right] \quad (12)$$

From (11), we know that $\tau_s^*(i)$ corresponds to T_{u_j}. Thus, $T_{u_j} = 1/\Delta f_j$ is obtained. Δf_j has a different value for each PU type as specified in standards and it is the input of the *PU Features Module*.

3.3 PU features module

As shown in Fig. 1, this module receives the PU activity index $\phi_j(i)$ and subcarrier spacing Δf_j and outputs a detailed description of the features of the identified PUs. $\phi_j(i)$ is useful for the definition of PU idle time and busy time, while Δf_j is used for the extraction of PU bandwidth and allowed interference threshold. In particular, Δf_j is compared with the known subcarrier spacing of PU standards to determine the corresponding PU standard. Once the standard has been identified, the values of the allowed interference threshold and bandwidth can be retrieved querying the REM. Based on this information, the CR will be able to efficiently vary its transmission parameters, and adapt its throughput as explained in the next section. The PU features are analyzed in the following.

3.3.1 Allowed PU interference threshold

Besides CR transmissions when PU is absent, we consider simultaneous CR and PU transmissions when a PU is present, provided that a tolerable interference level is satisfied. We define a PU allowed interference threshold I_j^{th} as the maximum interference power that can be tolerated by the *j*-th PU when there are simultaneous transmissions in the same band. I_j^{th} is used to adapt the CR transmission power, as it will be explained in the following Sect. 4.1.

3.3.2 PU bandwidth

An important parameter that the users of a CR network have to consider is the bandwidth of PUs. Each PU transmission band occupies a given bandwidth depending on the particular standard. In the following, the *j*-th band is referred to the band in which the *j*-th PU type is transmitting. In Sect. 4.2 the impact of the bandwidth on the CR throughput is discussed.

3.3.3 PU Idle/busy time

The transmission time allowed to a CR is related to the idle/busy time of the PUs. For this reason, an accurate

model of the PU activity is important. The PU activity index $\phi_j(i)$, described in Sect. 3.1, represents the traffic patterns at the i-th time sample on the j-th band where the j-th PU type is trasmitting. The PU arrival rate is defined equal to the activity index $\phi_j(i)$. Thus, the inter-arrival time corresponds to $1/\phi_j(i)$, which is the idle time T_j^{idle}, while the busy time T_j^{busy} is equal to $1/(1 - \phi_j(i))$.

4 Reconfigurability effects on CRs

Given the characterization of the specific PUs described above, in the following we describe how to adapt the CR parameters, i.e. transmission power, time and bandwidth, to achieve an adaptive interference protection towards PUs while efficiently increasing CR throughput.

4.1 CR adaptive parameters

The interaction between CR parameters and PU features is depicted in Fig. 2 showing that CR adaptability allows improvement in both frequency and time domains. For instance:

- Figure 2(a) shows the considered spectrum in a certain period of time. The spectrum is allocated to three different PUs, but in that period of time only PU_1 and PU_3 are active, while PU_2 is silent. Each PU occupies a given bandwidth and allows a certain interference threshold according to its transmission power. This threshold refers to the case of contemporary PU and CR transmissions in the same band.
  In Fig. 2(a), PU_1 transmits at a power level P_{PU_1} that is higher than the power level P_{PU_3} of PU_3, and the allowed interference threshold of PU_1 is higher than PU_3 in their respective bands. Consequently, in case of contemporary CR and PU transmissions, the CR transmission power must be set depending on the allowed interference thresholds of PUs in their respective bands, to assure interference protection towards PUs according to (13). In Fig. 2(a), $P_{1,\,CR}$ and $P_{3,\,CR}$ refer to the CR transmission power in the band of PU_1 and PU_3 respectively. As shown in Fig. 2(a), PU_2 is silent, thus the CR can transmit at the maximum power $P_{max,\,CR}$ in the band of PU_2.
- Figure 2(b) describes the behavior in the time domain of a CR transmitting in the band of PU_1. The CR changes its transmission power depending on the condition that PU_1 is present or absent, and the CR transmission time varies according to the PU_1 activity. If PU_1 has been detected, CR transmits simultaneously to PU_1 by setting its transmission power to $P_{1,\,CR}$, whose value depends on the interference threshold allowed by

(a) Frequency domain
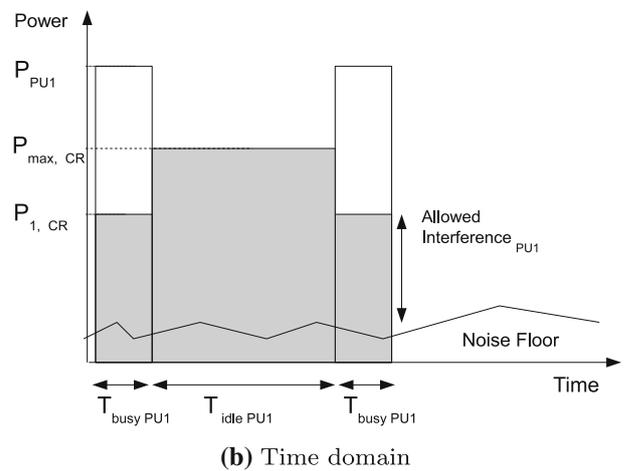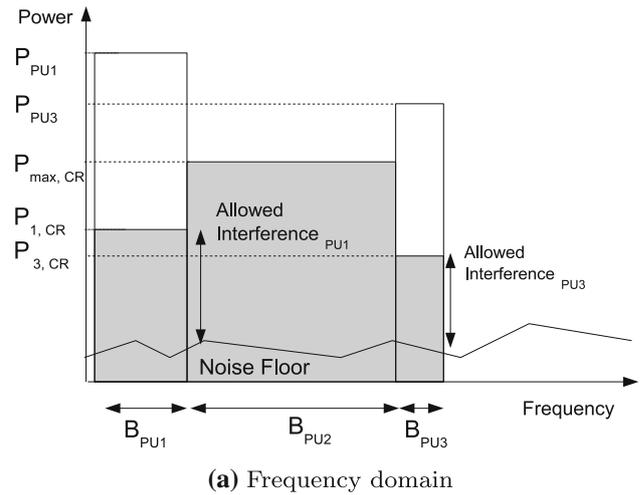
(b) Time domain

Fig. 2 PU features/CR parameters in frequency and time domain

PU_1, for a period of time equal to T_j^{busy} according to (14). If PU_1 has not been detected, CR transmits at its maximum power level $P_{max,\,CR}$, for a period of time equal to T_j^{idle} according to (14).

The CR parameters related to the features of heterogeneous PUs are reported in Table 1 and Fig. 1. Specifically we consider:

- PU allowed interference threshold/CR transmission power
- PU/CR bandwidth
- PU idle, busy time/CR transmission time

The CR parameters are listed hereafter.

4.1.1 CR transmission power

PU allowed interference thresholds I_j^{th} is defined as the interference received at PU device due to CR transmission.

Table 1 PU features vs CR adaptive parameters

Features of j-th PU type	CR parameters	CR adaptability effects
I_j^{th}	P_{tx}	CR throughput/ interference
B_j	B	CR throughput
T_j^{idle}, T_j^{busy}	$T_{tx}^{\max}$	CR throughput

Thus, CR transmission power P_{tx} of a CR that transmit on the band of the j-th PU type is set according to:

$$P_{tx} \le I_j^{\text{th}} \tag{13}$$

so that signal to interference plus noise ratio (SINR) of a PU device receiving CR interference respects predetermined values, according to the detected j-th PU type. SINR is defined as $P_{rx_j}/(I_j^{\text{th}} + N_0)$, where P_{rx_j} is the PU received power and N_0 is the noise power. Without loss of generality, we do not consider the channel effect between CR transmitter and PU reveir when calculating I_j^{th}. In fact, since there are contemporary PU and CR transmission in the same band, the possibility to cause interfence to PU when adjusting CR power is high. Thus, we prefer to set a lower value of threshold I_j^{th} instead of a higher one with the need of calculating the channel between CR and PU. In [12], imperfect channel information between CR transmitter and PU receiver is considered.

4.1.2 CR bandwidth

The available CR bandwidth varies according to the detected PU types. In particular, we consider a system where the spectrum is allocated to different PUs, which occupy different bandwidths. After classifying the PU types, the CR base station assigns to a specific CR the transmission frequency and bandwidth of the PU type that better meets its rate requirements.

4.1.3 CR transmission time

The maximum achievable value of CR transmission time is defined as:

$$T_{tx}^{\max} = \begin{cases} T_j^{idle} = \frac{1}{\phi_j(i)} & H_0 \\ T_j^{busy} = \frac{1}{1 - \phi_j(i)} & H_1 \end{cases} \tag{14}$$

where $T_{tx}^{\max}$ is the maximum transmission time of a CR that transmits on the spectrum band of the j-th PU type. Thus, when the j-th PU type is not detected (case H_0), $T_{tx}^{\max}$ depends on T_j^{idle} and it is inversely proportional to the activity index of the PU transmitting in that band. In fact, in a CR network, it is reasonable to assume that CR transmission time is short with respect to the idle time [8].

When the j-th PU type is detected (case H_1), we also consider contemporary PU and CR transmissions, thus, the maximum value of $T_{tx}^{\max}$ is set equal to T_j^{busy}. In the latter case the CR transmission power P_{tx} is set according to (13) to provide interference protection towards PU.

4.2 CR throughput adapter

Here we explain how to exploit the features of heterogeneous PUs to improve CR adaptability.

In the following, we suppose that the j-th PU type has been detected and its features are used to adapt the throughput of a CR in different scenarios.

Let the period $T_{tot} = T_{tx} + T_s$ denote CR transmission plus sensing time. Specifically, the sensing time T_s is equal to $T_c + T_r$, where T_c is the time useful to detect and classify PUs, and T_r is the time required for consulting the REM in order to recover the values of PU features.

We express the achievable throughput R in the period T_{tot} as:

$$R = R_1 + R_2 + R_3 \tag{15}$$

where:

- The first term refers to the situation in which the PU is absent and the CR correctly detects the idle state without false alarm.
- The second term takes into account the scenario in which the CR detects the PU correctly and transmits/ coexists with it.
- The third term refers to the case when the PU is present, but the CR detector fails and causes interference towards the PU.

R_1 is given by

$$R_1 = \frac{T_{tx}}{T_{tx} + T_s} C_1 (1 - \bar{P}_f) P_{idle} \tag{16}$$

where the term $\frac{T_{tx}}{T_{tx}+T_s}$ is the CR efficiency expressed as the ratio between the CR transmission time and the transmission plus sensing time. The maximum value of T_{tx} is equal to $1/\phi_j(i)$, given by (14) in case H_0 holds. The term C_1 represents the achievable capacity in the first case. $(1 - \bar{P}_f) P_{idle}$ is the probability of the occurrence of the first scenario, i.e. the probability P_{idle} that the PU is absent, given in (4), multiplied by the probability $(1 - \bar{P}_f)$ that CR detects the idle state without false alarm. The capacity C_1 may be expressed as

$$C_1 = \frac{B}{N} \sum_{k=1}^{N} \log_2 \left(1 + \frac{P_{tx}^{\max} |H_k|^2}{N_0 \frac{B}{N}} \right) \tag{17}$$

where B is the bandwidth assigned to the CR allowed to transmit on the j-th PU band. N is the number of subcarriers

allocated to the CR. The wireless channel is modeled as frequency selective fading and H_k is the channel gain of the k-th subcarrier. AWGN is present with noise power spectral density (PSD) equal to $N_0/2$ for all subcarriers of all users. The transmission power of the CR is set to the maximum value $P_{tx}^{\max}$ since this term refers to the case of correct detection of the idle state.

The second term R_2 in (15) is defined as follows

$$R_2 = \frac{T_{tx}}{T_{tx} + T_s} C_2 \bar{P}_d P_{busy} \qquad (18)$$

C_2 is the achievable capacity in the second case. The product $\bar{P}_d P_{busy}$ is the probability that the second case happens, that is the probability P_{busy} that a PU is transmitting, given in (3), multiplied by the probability $\bar{P}_d$ that the CR correctly detects the PU. In this case, the maximum value of T_{tx} is equal to $1/(1 - \phi_j(i))$, according to (14) in case H_1. C_2 is expressed as

$$C_2 = \frac{B}{N} \sum_{k=1}^{N} \log_2 \left(1 + \frac{P_{tx}|H_k|^2}{I + N_0 \frac{B}{N}} \right) \qquad (19)$$

where CR transmission power P_{tx} is calculated using (13). In this case, the PU interference power I measured at CR is added to the thermal noise. We have simultaneous PU and CR transmissions in the same band and I takes into account the interference suffered by CR.

The third term in (15) is defined as

$$R_3 = \frac{T_{tx}}{T_{tx} + T_s} C_3 (1 - \bar{P}_d) P_{busy} \qquad (20)$$

where $(1 - \bar{P}_d)P_{busy}$ is the probability that the third situation happens, i.e. the probability P_{busy} that the spectrum is occupied by a PU multiplied by the probability $(1 - \bar{P}_d)$ that the CR will not detect it. CR transmits at the maximum transmission power $P_{tx}^{\max}$ causing interference towards PU. The maximum value of T_{tx} is equal to $1/\phi_j(i)$, according to (14) in case H_0. The capacity C_3 is expressed as

$$C_3 = \frac{B}{N} \sum_{k=1}^{N} \log_2 \left(1 + \frac{P_{tx}^{\max}|H_k|^2}{I + N_0 \frac{B}{N}} \right) \qquad (21)$$

We have $C_1 > C_3 > C_2$. First of all, $C_1 > C_3$. In fact, (21) is similar to (17) but there are simultaneous PU and CR transmissions and the term I takes into account the PU interference suffered by CR. Then, $C_3 > C_2$ because CR transmission power P_{tx} in (19) is limited by the allowed interference thresholds I_j^{th}, as shown in (13).

Finally, we report some considerations about the time T_c to detect and classify PUs and the sensing time T_s that is directly related to T_c, being $T_s = T_c + T_r$. While for a given T_{tx}, a longer T_c gives a lower coefficient $\frac{T_{tx}}{T_{tx}+T_s}$, for a given probability of detection, a longer T_c corresponds to a

lower probability of false alarm. This is the case in which a CR has a higher probability of using the channel. In fact, T_c, and thus T_s, is related to P_d and P_f of the CF detector/classifier proposed in Sect. 3.2.

5 Performance evaluation

The performance of the proposed $(CR)^2$ framework is evaluated by separately analyzing the behavior of the CF detector/classifier and the CR throughput adapter.

5.1 Simulation environment

All simulation results have been obtained using MATLAB. The modeled system is composed of several PU types which use OFDM transmission, and a CR centralized entity that stores the values of PU features in a REM. A CR, after detecting PUs, consults the REM to extract the value of their features for throughput adaptation.

We consider the following PU standards: 802.11, 802.16e and DVB-T 2K mode. The PU parameters are summarized in Table 2. In particular, the activity index, bandwidth and allowed interference threshold are used to evaluate the CR adaptive throughput in Sect. 5.3.

Regarding the values of PU features shown in Table 2, we take into account different interference thresholds I_j^{th} allowed by PU standards. The mean value of the PU activity index $\overline{\phi}_j$, defined in Sect. 3.1, is randomly distributed between 0.1 and 0.4 [3]. The bandwidth B_j for each PU is obtained by $N_j \times \Delta f_j$, where N_j is the FFT size and Δf_j is the subcarrier spacing.

The wireless channel is modeled as fading multipath with an exponential power profile. The delay spread is set equal to 4 μs. Without loss of generality, the subchannel gains are known at CR receiver when calculating CR throughput expressed in (15), since they can be estimated using known techniques [7].

5.2 CF detector/classifier

The performances of the CF detector/classifier are analyzed by showing the probability of false alarm P_f and missed detection P_{md} of the detector/classifier in Fig. 3(a), (b).

Table 2 PU features

PU standard /PU features	802.11	802.16	DVB
FFT	64	512	2,048
I_j^{th}	0.9 pW	9.9 pW	31.5 pW
B_j	20 MHz	5 MHz	8 MHz
$\overline{\phi}_j$	0.4	0.3	0.1

Figures 3(a), (b) shows the probability of false alarm P_f and missed detection P_{md} of the CF detector/classifier. As explained in Sect. 3.2, the developed MAP detector requires P_{busy} and P_{idle}, which are set to 0.63 and 0.37 according to [3]. The term ϵ of the threshold λ in (7) is chosen to obtain P_f equal to 0.1 in case of DVB PU signal. As shown in Fig. 3(b), the DVB PU signal can be easily detected for an (E_b/N_0) lower than the (E_b/N_0) required for both 802.16 and 8021.11 PU signals.

5.3 CR throughput adapter

In the following, the performance of the CR throughput adapter is considered. Specifically, in Sect. 5.3.1 CR throughput is analyzed by varying PU allowed interference

thresholds, in Sect. 5.3.2 by varying PU bandwidth, in Sect. 5.3.3 by varying PU activity index, and finally in Sect. 5.3.4 by considering the combined effect of all the features.

In the last Sect. 5.3.4, we compare the performance of CR throughput by using or not the REM. In particular, we made the assumption that, in case we use the REM, after the detection and classification of heterogeneous PUs we are able to extract the PU features stored in the REM. On the contrary, without using the REM, we are not able to recover the value of the PU features, thus we consider to use the minimum value of those features in order to avoid interference towards all types of PUs.

5.3.1 Allowed interference threshold

Figure 4 shows the behavior of the term C_2 expressed in (19), normalized to the transmission bandwidth, depending on various interference thresholds allowed by different PU standards.

The interference I_j^{th}, allowed by a PU device receiving CR interference, are set equal to 0.9, 9.9 and 31.5 pW respectively. As shown in Table 2, these values correspond to the 802.11, 802.16 and DVB PU standards. The received PU power level is set to the typical value of 100 pW. We set the noise power to the usual value 0.1 pW for a bandwidth of 20 MHz.

Under this hyphotesis, the SINR is easily calculated starting from PU interference thresholds. In particular, the chosen interference thresholds 0.9, 9.9 and 31.5 pW correspond to SINR of a PU device receiving CR interference equal to 20, 10, and 5 dB respectively. Moreover, the interference threshold values are used to calculate CR

(a) Probability of false detection
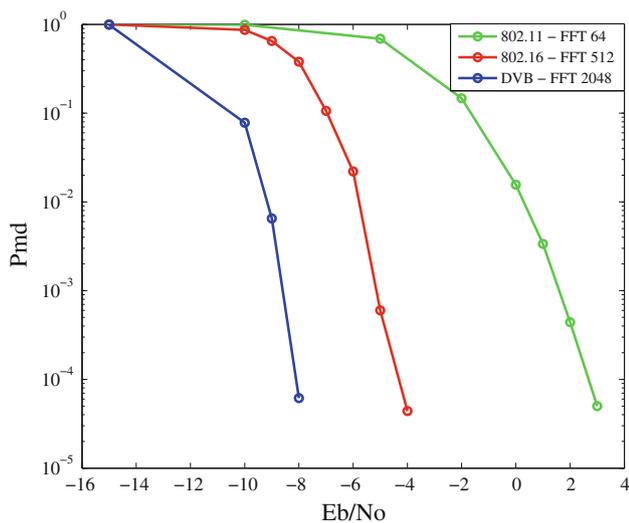
(b) Probability of missed detection

Fig. 3 Performance of CF detector/classifier
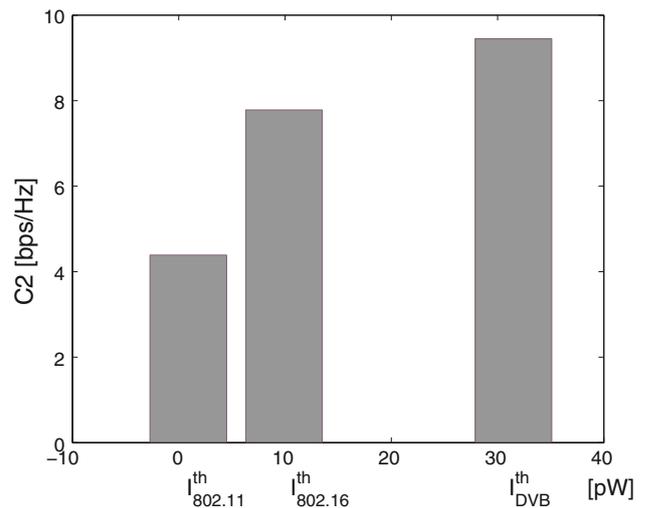
Fig. 4 Effects of the PU allowed interference thresholds: C_2 versus interference thresholds

transmission power P_{tx} according to (13). Without loss of generality, in our work, we do not consider the path loss in the signal strength. Thus, we suppose that these values are the same of the CR transmission power levels P_{tx}, which are then used in (19) to calculate C_2. Furthermore in (19), the interference I that a PU transmission causes to the CR is set equal to 2 pW.

When a CR does not detect any PU signal, it uses the maximum transmission power P_{tx}^{max} set to 50 mW. Thus, C_1, normalized to the bandwidth in (17), becomes equal to 38.7, while the normalized C_3 in (21) is 34.3.

5.3.2 Bandwidth

Figure 5(a), (b) show the behavior of C_1, C_2, C_3 expressed in (17), (19), (21) varying the bandwidth B_j: 5 MHz bandwidth if a 802.16e PU signal has been detected, 8 MHz for DVB PU signal, and 20 MHz for 802.11a PU signal, as summarized in Table 2. Figure 5(a) shows that the non-normalized capacity terms in (17), (19), (21) increase with the bandwidth, while Fig. 5(b) reveals that the capacity terms normalized to the bandwidth decrease with the increase of the bandwidth.

5.3.3 Activity index

As explained in Sect. 4.1.3, the maximum CR transmission time T_{tx}^{max} is equal to PU idle time T_j^{idle} when a PU is not detected, or it is equal to PU busy time T_j^{busy} when a PU is detected. T_j^{idle} and T_j^{busy} depend on $\overline{\phi}_j$. Using (14), we set the value of T_{tx}^{max} equal to T_j^{idle} (case H_0) in (16) and (20), and equal to T_j^{busy} (case H_1) in (18). In this way, we can calculate the CR throughput R as expressed in (15).

Equation (15) also needs the values of the sensing time T_s, the bandwidth B, and the interference threshold I_j^{th}. The sensing time T_s is equal to $T_c + T_r$, where T_c is the time necessary to detect and classify different PUs, and T_r is the time required to recover the values of the PU features from the REM. T_c is set equal to 5 OFDM symbol time that, for FFT size of 2,048 and guard interval equal to $T_u/4$ with $t_s = 0.1$ μs, corresponds to 1.28 ms, while T_r is set equal to 160 ms, equal to the LTE delay budget. We consider a bandwidth of 20 MHz and an interference threshold I_j^{th} equal to 31.5 pW, so that C_1, C_2 and C_3 are equal to 38.7, 9.4 and 34.3, as calculated in Sect. 5.3.1. P_f and P_d are set to reasonable values of 0.1 and 0.95 respectively, while P_{busy} is set to [0.63 0.64 0.65 0.66] and P_{idle} is set to [0.37 0.36 0.35 0.34], as in the simulation results in [3].

Figure 6 shows how the value of R expressed in (15) varies depending on the value of $\overline{\phi}_j$.
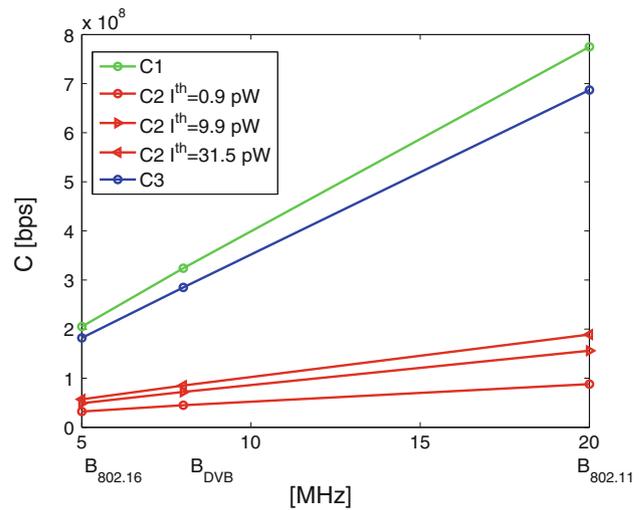
(a) Non-normalized Capacity terms vs Bandwidth
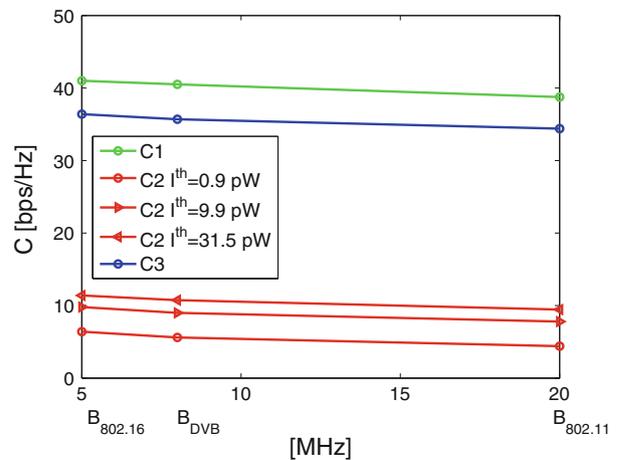
(b) Normalized Capacity terms vs Bandwidth

Fig. 5 Effects of the PU bandwidth: capacity terms versus bandwidth

5.3.4 Effects of the combined PU features

Figure 7 shows the effects of the PU features on CR throughput R expressed in (15), which is normalized to the bandwidth.

When the REM is not used, the time T_r to recover the PU features from the REM is equal to zero, thus increasing the CR throughput R. However, without REM, it is not possible to extract the exact value of the features of heterogeneous PUs, thus, the value of the features is set to the minimum value in order to avoid interference towards each type of PU. Specifically, the bandwidth is set equal to 5 MHz, the mean value of the activity index $\overline{\phi}_j$ is set to 0.4 and a null value is considered for the interference threshold I_j^{th} allowed by the PU. In other words, the term C_2 does not
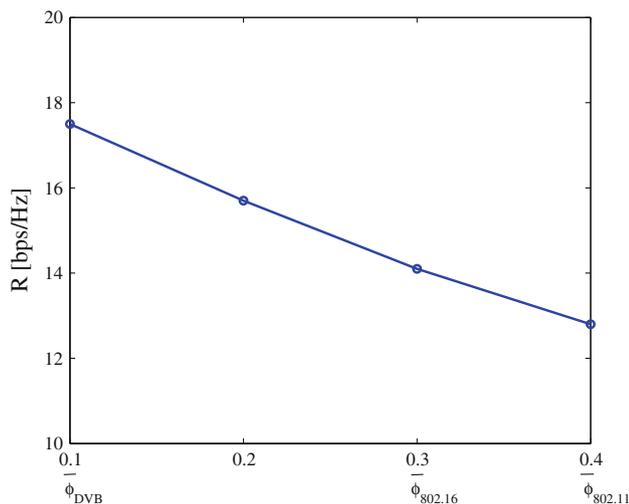
Fig. 6 Effects of the PU activity index: throughput versus activity index
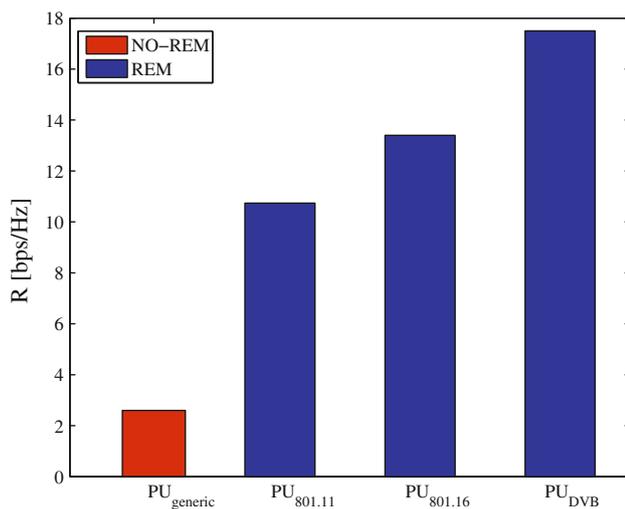
Fig. 7 Combined effects of all the features of the detected PUs: normalized throughput

contribute to the calculation of R in (15) in case the REM is not used.

As shown in Fig. 7, there is a benefit in using the REM and, among all types of PUs, DVB signal is the PU type that allows the maximum normalized CR throughput.

6 Conclusion

In this paper, we have proposed the characterization of heterogeneous PUs to improve CR reconfigurability in terms of interference and throughput adaptability. PUs characterization consists in a detector/classifier that distinguishes

different PUs. Their features, i.e. the allowed interference levels, the bandwidth and the idle/busy time, are stored in a REM and they are exploited by the CR interference/throughput adapter to improve CR performance.

The proposed solution is evaluated by showing the false alarm and missed detection probability of the detector/classifier in multipath fading channel with AWGN. Moreover, the CR throughput is analyzed by varying each PU feature separately. By considering the combined effects of all the PU features, we show that DVB signal is the PU type that allows the maximum normalized CR throughput. Simulation results confirm that CR throughput is efficiently adapted according to the features of the detected PU types.

References

1. Akyildiz, I. F., Lee, W.-Y., Vuran, M. C., & Mhanty, S. (2006, September). Next generation/dynamic spectrum access/cognitive radio wireless networks: A survey. *Computer Networks, Elsevier, 50*(13), 2127–215.
2. Bixio, L., Oliveri, G., Ottonello, M., & Regazzoni, C. S. (2009). OFDM recognition based on cyclostationary analysis in an Open Spectrum scenario. *IEEE 69th Vehicular Technology Conference*, April 26–29.
3. Canberk, B., Akyildiz, I. F., & Oktug, S. (2011, February). Primary user activity modeling using first-difference filter clustering and correlation in cognitive radio networks. *IEEE/ACM Transactions on Networking, 19*(1), 170–183.
4. FCC. (2002). Spectrum policy task force report. ET Docket no. 02-135.
5. FCC. (2003, December). Notice of proposed rule making and order. ET Docket, no. 03-222.
6. Goh, L. P., Lei, Z., & Chin, F. (2007, June 24–28). DVB detector for cognitive radio. *IEEE international conference on communications, ICC 2007*.
7. Hu, D., & He, L. (2010, December 6–10). Pilot design for channel estimation in OFDM-based cognitive radio systems. *IEEE international conference on communications, ICC 2010*, pp.1–5.
8. Lee, W.-Y., & Akyildiz, I. F. (2008, October). Optimal spectrum sensing framework for cognitive radio networks. *IEEE Transaction on Wireless Communications, 7*, 3845–3857.
9. Liu, H., Yu, D., & Kong, X. (2009, April 26–29). A new approach to improve signal classification in low SNR environment in spectrum sensing. *IEEE 69th vehicular technology conference, VTC Spring 2009*.
10. Mishra, S. M., Sahai, A., & Brodersen, R. W. (2006, June). Cooperative sensing among cognitive radios. In *Proceedings of the IEEE ICC 2006, 4*, 1658–1663.
11. Muraoka K., Ariyoshi, M., & Fujii, T. (2008, October 14–17). A novel spectrum-sensing method based on maximum cyclic autocorrelation selection for cognitive radio system. *IEEE symposium on new frontiers in dynamic spectrum access networks, DySPAN 2008*.
12. Musavian, L., & Aissa, S. (2009). Fundamental capacity limits of cognitive radio in fading environments with imperfect channel

information. *IEEE Transaction on Wireless Communication,* *57*(11), 3472–3480.

13. Proakis, J. G. (2001). *Digital communications* (2nd Edn.). New York: McGraw-Hill.

14. Shellhammer, S. J. (2008, June 9–10). SPECTRUM SENSING IN IEEE 802.22. *IAPR workshop on cognitive information processing, 2008*, Santorini, Greece.

15. da Silva, C. R. C., Brian, C., & Kim, K. (2007, January 29–2007, Febraury 2). Distributed spectrum sensing for cognitive radio systems. *Information theory and applications workshop, 2007*, pp. 120–123.

16. Stevenson, C. R., Cordeiro, C., Sofer, E., & Chouinard, G. (2005, September). Functional requirements for the 802.22 WRAN standard. IEEE 802.22-05/0007r46.

17. Sutton, P., Nolan, K., & Doyle, L. (2008, January). Cyclostationary signatures in practical cognitive radio applications. *IEEE Journal on Selected Areas in Communications, 26*, 13–24.

18. Vizziello, A., Akyildiz, I. F., Agustí, R., Favalli, L., & Savazzi, P. (2010, December 6–10). OFDM signal type recognition and adaptability effects in cognitive radio networks. In *Proceedings of IEEE GLOBECOM 2010*, Miami, Florida, USA.

19. Vizziello, A., & Perez-Romero, J. (2011, Ocotober 26–29). System architecture in cognitive radio networks using a radio environment map. In *Proceedings of CogART 2011, (invited paper)*, Barcelona, Spain.

20. Wang, B., & Liu, K. J. R. (2011, Febraury). Advances in cognitive radio networks: A survey. *IEEE Journal of Selected Topics in Signal Processing, 5*(1), 5–23.

21. Zhao, Y., Morales, L., Gaeddert, J., Bae, K., Um, J.-S., & Reed, J. (Apr. 2007). Applying radio environment maps to cognitive wireless regional area networks. In *Proceedings of IEEE DySPAN 2007*, pp. 115–118.

Author Biographies

Anna Vizziello received the Laurea degree in Electronic Engineering and the Ph.D. degree in Electronics and Computer Science from the University of Pavia, Italy, in 2007 and in 2011, respectively. She is currently a Post Doc researcher in the Telecommunication and Remote Sensing Laboratory at the University of Pavia, Italy. From 2007 to 2009 she also collaborated with European Centre for Training and Research in Earthquake Engineering (EUCENTRE) working in the Telecommunications and Remote Sensing group. From 2009 to 2010 she has been a visiting researcher at Broadband Wireless Networking Lab at Georgia Institute of Technology, Atlanta, GA. In summer 2009 and 2010 she has also been a visiting researcher at Universitat Politècnica de Catalunya, Barcelona, Spain. Her research interests are Broadband Transmission Systems and Cognitive Radio Networks.

Ian F. Akyildiz received the B.S., M.S., and Ph.D. degrees in Computer Engineering from the University of Erlangen-Nurnberg, Germany, in 1978, 1981 and 1984, respectively. Currently, he is the Ken Byers Chair Professor in Telecommunications with the School of Electrical and Computer Engineering, Georgia Institute of Technology, Atlanta, the Director of the Broadband Wireless Networking Laboratory and Chair of the Telecommunication Group at Georgia Tech. Dr. Akyildiz is an honorary professor with the School of Electrical Engineering at Universitat Politècnica de Catalunya (UPC) in Barcelona, Catalunya, Spain and founded the N3Cat (NaNoNetworking Center in Catalunya). He is also an honorary professor with the Department of Electrical, Electronic and Computer Engineering at the University of Pretoria, South Africa and the founder of the Advanced Sensor Networks Lab. Since 2011, he is a Consulting Chair Professor at the Department of Information Technology, King Abdulaziz University (KAU) in Jeddah, Saudi Arabia. Since September 2012, Dr. Akyildiz is also a FiDiPro Professor (Finland Distinguished Professor Program (FiDiPro) supported by the Academy of Finland) at Tampere University of Technology, Department of Communications Engineering, Finland. He is the Editor-in-Chief of Computer Networks (Elsevier) Journal, and the founding Editor-in-Chief of the Ad Hoc Networks (Elsevier) Journal, the Physical Communication (Elsevier) Journal and the Nano Communication Networks (Elsevier) Journal. He is an IEEE Fellow (1996) and an ACM Fellow (1997). He received numerous awards from IEEE and ACM. His current research interests are in nanonetworks, Long Term Evolution (LTE) advanced networks, cognitive radio networks and wireless sensor networks.

Ramon Agustí received the Engineer of Telecommunications degree from the Universidad Politécnica de Madrid, Spain, in 1973, and the Ph.D. degree from the Universitat Politècnica de Catalunya (UPC), Spain, 1978. He became Full Professor of the Department of Signal Theory and Communications (UPC) in 1987. After graduation he was working in the field of digital communications with particular emphasis on transmission and development aspects in fixed digital radio, both radio relay and mobile communications. For the last twenty years he has been mainly concerned with aspects related to radio resource management in mobile communications. He has published about two hundred papers in these areas and co-authored three books. He participated in the European program COST 231 and in the COST 259 as Spanish representative delegate. He has also participated in the RACE, ACTS and IST European research programs as well as in many private and public funded projects. He

received the Catalonia Engineer of the year prize in 1998 and the Narcis Monturiol Medal issued by the Government of Catalonia in 2002 for his research contributions to the mobile communications field. He is a Member of the Spanish Engineering Academy.

Lorenzo Favalli graduated in Electronic Engineering form Politechnic of Milano in1987 and obtained the PhD from the same university in 1991. Since 1991 he is with the University of Pavia first as Assistant Professor and, from 2000 as Associate Professor. During his career Dr. Favalli has been recipient of several prizes, such as the grant from SIP (now Telecom Italia) for his graduation thesis titled "Telephone service on the C-NET local area network". The same work won the 1987 "Oglietti" prize from AEI-CSELT as the best thesis work on communication and switching. In 1989 obtained a AEI-ISS grant and spent about one year as a visiting scientist at the Computer Communications Research Center of the Washington University in St. Louis (USA). In 1988 he also won the special prize at the international contest "Computer in the Cathedral" sponsored by NCR and International Cathedral Association developing a multimedia hypertext system for the fruition of cultural heritage. He is a member of the commission for Distance Learning activities of the Faculty of Engineering and has served as the head of the Scientific Board of the Engineering Library and he is still a member of the board. He has participated in many research projects funded by public institutions (MIUR- PRIN and FIRB projects) and private companies (STmicroelectronics, Ericsson, Alenia, Marconi). His research activity has covered various aspects of signal analysis, in particular video, and transmission in both wireless and wired networks.

Pietro Savazzi received the Laurea degree in Electronics Engineering from the University of Pavia in 1995. In 1999 he obtained the Ph.D. in Electronics and Computer Science from the same University and then he joined Ericsson Lab Italy, in Milan, as a system designer, working on broadband microwave systems. In 2001 he moved to Marconi Mobile, Genoa, Italy, as a system designer in the filed of 3G wireless systems. Since 2003 he has been working at the University of Pavia where he is currently teaching, as an assistant professor, two courses on signal processing and digital communications. His main research interests are in wireless systems.